Resource-Aware Relay Selection for Inter-Cell Interference Avoidance in 5G Heterogeneous Network for Internet of Things Systems

Nhu-Ngoc Dao[a], Minho Park[b], Joongheon Kim[a], Jeongyeup Paek[a], Sungrae Cho[a,*]

[a]*School of Computer Science and Engineering, Chung-Ang University, Republic of Korea*
[b]*Department of ICMC Convergence Technology, Soongsil University, Republic of Korea*

Abstract

The fifth-generation (5G) heterogeneous networks (HetNets) are gaining attention to be a key enabler that provides promising infrastructure for the massive proliferation of Internet of Things (IoT) devices and their services. However, one of the key challenges that the IoT terminals face is the inter-cell interference (ICI) problem since the 5G HetNets are generally deployed based on a co-channel model that overlays numerous pico eNodeBs (eNBs) on top of macro eNBs grid on the same frequency band. In order to overcome the ICI problem, we propose a relay-assisted communication approach by which the data of interfered IoT terminal (iIT) in the ICI area is relayed, via a device-to-device connection, to its neighboring IoT terminals which has good signal to and from the network. The key component in this proposed scheme is the relay selection algorithm which aims at maximizing the network resource availability at the highest priority, as well as device data rate. Firstly, resource availability maximization (RAmax) function determines an eNB that has maximum resource availability among all neighboring eNBs of the iIT to be a gateway node for the relay connection to the network (referred to as reNB). Among the IoT terminals associated with the reNB, a relay IoT terminal (called rIT) linking iIT and reNB is selected by a condition of maximum channel quality to the reNB. Simulation results show that our proposed algorithm increases total network throughput and the number of simultaneously served ITs by 44% and 20%, respectively.

Keywords: Internet of Things, 5G Heterogeneous Network, Inter-Cell Interference, Network resource availability, Device-to-device communication

1. Introduction

A typical fifth-generation (5G) heterogeneous networks (HetNets) comprise a grid of macro eNodeBs (MeNBs) which are well spectrum allocated and deployed for a wide-area coverage purpose. Within each MeNBs coverage, pico eNodeBs (PeNBs) are introduced to complement coverage black-holes uncovered by the MeNBs, and also enhance local user equipments (UEs) throughput. This model is depicted in Figure 1. Moreover, the MeNB and PeNBs utilize the same frequency channels for data transmission according to the co-channel deployment model due to spectrum scarcity. Within this scenario, dedicated signaling channels are assigned to the MeNBs for management and control operations serving both MeNBs and PeNBs.

By utilizing this 5G HetNets infrastructure, Internet of Things (IoT) systems are expected to gain better connectivity and spread services over more geographical areas at economically feasible costs. However, although the 5G HetNets provide a significant network throughput improvement over its predecessors, the negative impact of this co-channel design is still an open issue which is known to be potential inter-cell interference (ICI) among eNBs (i.e., MeNBs and PeNBs) [1]. IoT terminals (ITs) are often based on resource-constrained platforms, and thus are sensitive to, and will suffer severely from, inter-cell interference. Therefore, the ITs located at the edges of PeNBs' coverage might suffer from poor signal-to-noise ratio (SNR) caused by ICI problem between MeNBs and PeNBs. It creates a likely annulus-shaped interference zone around each PeNB. When an IT locates in these ICI areas, the channel quality degrades rapidly. As a result, the transmission rate

*Corresponding author
Email addresses: dnngoc@uclab.re.kr (Nhu-Ngoc Dao), mhp@ssu.ac.kr (Minho Park), joongheon@cau.ac.kr (Joongheon Kim), jpaek@cau.ac.kr (Jeongyeup Paek), srcho@cau.ac.kr (Sungrae Cho)

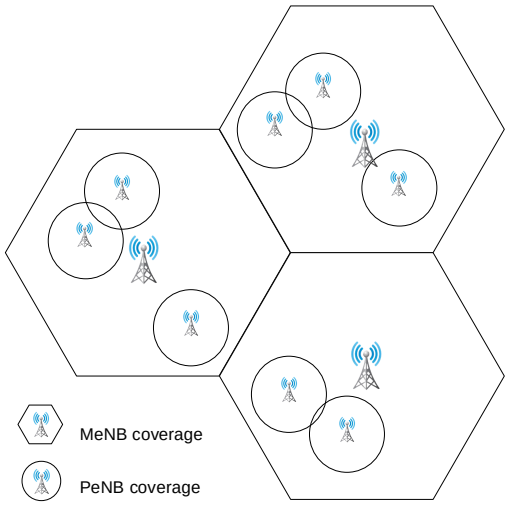

Figure 1: An example deployment scenario of a 5G heterogeneous network (HetNet) with macro eNodeBs (MeNBs) and pico eNodeBs (PeNBs).

may fall to a very low-rate level. In the worst case, it may introduce wireless connection loss between the IT and eNBs.

Among existing solutions which have been proposed in order to mitigate the ICI problem, most of the solutions have generally attempted to balance resource usage and allocation between MeNBs and PeNBs to reduce interference intensity. In other words, simultaneous throughput improvements for both MeNBs and PeNBs are not possible at the same point in time. For instance, an almost blank subframe (ABS) technique [2] works with the concept that the PeNBs gain their coverages and provide more throughput for its associated devices if and only if the corresponding MeNB turns off or reduces its transmit power. Moreover, since IoT systems may comprise of lightweight terminals based on resource-constrained platforms with limited capabilities (e.g. data rate, computation, memory, energy budget, etc.), existing techniques aiming at high data-rate LTE user equipments may not be applicable [3].

Unlike prior approaches, our solution aims at supporting the IoT systems by utilizing relay-assisted communication via device-to-device (D2D) connection that is expected to be popularized among ITs in the IoT era [4]. A prime example of this approach is the device relaying with operator controlled (DR-OC) model proposed by Tehrani *et al.* [5] which utilizes the D2D communication standardized in 3GPP TR 22.803 [6]. In the DR-OC model, *a device at the edge of an eNB or in a poor coverage area can communicate with the eNB by relaying its information via other devices. The operator communicates with the relaying devices for partial or full control link establishment*. This approach has some advantages over the other techniques as follows. First, it resolves the problem where ITs are in poor SNR areas without any directly negative impacts on the other ITs or eNBs. Second, the ITs with poor signals (referred to as iIT) are able to increase their throughput and reduce the transmit power by relaying data through a D2D connection. In addition to many advantages, the model exposes some ambiguities that must be addressed sufficiently before it can be used for potential applications in a real scenario. Especially, the algorithms and criteria for determining the relay IT (called rIT) and relay eNB (referred to as reNB) are crucial for an effective relay-assisted communication.

In this paper, we develop a novel algorithm in order to complement the DR-OC model for determining an appropriate pair of rIT and reNB for an iIT. The decision criteria are based on two objectives in a descending order: (i) maximizing network resource availability, by which a large number of new iITs can be served by the network; and (ii) maximizing the throughput of the iITs. Under these criteria, the proposed resource availability maximization (RAmax) function determines an eNB that has maximum resource availability among the neighboring eNBs of iIT to be a gateway node for the relay connection to the network. The resource availability is defined as maximum time interval during which an eNB still has sufficient resources to serve a newly incoming device. Among the ITs associated with the reNB, a rIT linking iIT and reNB is selected by a condition of maximum channel quality to the reNB. As a result, a relay connection is established for the iIT going through rIT and reNB to reach the network instead of direct poor-quality channels caused by ICI. With the aforementioned objectives, our scheme supports significant number of iITs with better throughput improvement and power consumption.

Our contributions in this paper are summarized as the followings:

- We have categorized the existing prior work on ICI mitigation techniques in 5G HetNets and identified their limitations. The taxonomy is based on the domains where the solutions are utilized including frequency-based, time-based, space-based, transmit power-based, and hybrid approaches (see Section 2).
- We have described a system model for 5G HetNet based IoT systems under typical assumptions. Based on this model, we proposed a novel relay

selection procedure that assists iITs to escape from ICI problem (see Section 3).

- To support the aforementioned relay selection, we have proposed a resource availability maximization (RAmax) function which utilizes M/M/1/K/FCFS queuing model to determine the most appropriate pair of reNB and rIT for the relay-assisted connection from iIT to the network (see Section 4).
- We have shown that the proposed scheme outperforms the existing techniques in terms of total network throughput, device energy consumption, resource allocation, and channel coding rate (see Section 5).

We discuss the advantages and drawbacks of the proposed solution in Section 6, then concludes the paper in Section 7.

2. Related work

Interference mitigation techniques have traditionally been one of the major research issues in wireless networks (e.g., [2, 7, 8, 9, 10, 11, 12, 13, 14, 15, 16, 17, 18, 19]). There have also been a significant number of research aiming at 5G HetNets. In this section, we categorize the existing solutions for ICI mitigation into (1) frequency-based, (2) time-based, (3) space-based, (4) power-control-based, and (5) hybrid approaches, and provide a taxonomy of the related work.

The frequency-based approach are techniques that arrange the frequency spectrum in a way to minimize overlapped areas among the assigned channels based on its geometry and function. In the frequency-based approach, one of the most popular techniques is fractional frequency reuse (FFR). FFR has been applied early in mobile networks as a typical method to mitigate the inter-cell interference problem, wherein the eNBs are partitioned into non-overlapped regions by using different frequency among neighboring eNBs. Although FFR is not a new approach, it is still effective in recent mobile generations and is continuously being developed. The popular FFR techiques include strict FFR, soft FFR, FFR-3, and optimal static FFR (OSFFR) algorithms [2, 16, 18]. Ever since the development of LTE systems, the network uses additional channel aggregation (CA) techniques to improve the total throughput and reduce the negative effects of inter-cell interference. The full spectrum is divided into two parts, named primary and secondary frequencies, respectively. Normally, the MeNB serves as the primary eNB which uses the primary frequency to transmit control and signaling information to all users in the control channel and also supports data connection within a limited bandwidth data channel. In addition, the PeNBs act as secondary eNBs which use the entire secondary frequency to transmit users data in higher throughput [10]. In the frequency-based approach, the network must balance frequency assignment among eNBs within a limited licensed spectrum. This approach cannot utilize full advantage of co-channel deployment.

The time-based approach focuses on scheduling the radio resources and transmissions in order to reduce the contention probability in the transmission environment. The time-based approach includes two subbranches: subframe alignment and modulation shifting techniques. The subframe alignment approach restricts or reduces transmission of the main ICI originator among eNBs (usaully MeNBs) in certain subframes. In case that the MeNB stops or reduces its transmission power, ICI is significantly reduced giving the PeNBs a chance to extend the eNB range and transmit at a higher data rate. Two prime examples of this approach are almost blank subframe (ABS) and reduced power ABS (RP-ABS), which have been used in LTE-A networks since the 3GPP Rel.10 standards [8, 15]. Within the modulation shifting techniques, the orthogonal frequency division multiplexing (OFDM) symbol shifting method is a prime example. In the OFDM symbol shifting technique, the subframe chain of PeNBs are shifted or even muted on the physical downlink shared channel (PDSCH) by some symbols to guarantee that the physical downlink control channel (PDCCH) of the MeNB/PeNBs do not interfere with the PeNBs/MeNB's CRS or control channel [7, 17]. Time-based approaches try to cut off the interference from the main generator when the victim eNB needs to transfer burst traffic or important data. Again, the network resource (i.e., time) is the trade-off point and the throughput of all eNBs cannot be improved simultaneously.

The space-based approach is a scheme in which multiple transmit and receive antennas at different locations are coordinated to provide better network and/or device throughput, especially in inter-cell interference area. The prime example of space-based approach is the coordinated multi-point (CoMP) technique. The principle of CoMP is to implement multiple transmit and receive antennas at different geographic locations to improve cell-edge UE experience. CoMP algorithms include coordinated beam-switching (CBS-CoMP), coordinated scheduling (CS-CoMP), joint transmission (JT-CoMP) and dynamic point selection (DPS-CoMP) [11, 13, 14, 19]. In a 5G HetNet, massive MIMO is expected

to provide high data rate connections for multiple users, and will be a good target environment for the CoMP to be deployed widely in real. Although this approach obtains promising results for the inter-cell interference problem, it is characterized by complicated deployment and maintenance.

In power-control based approach, the transmission power is balanced and scheduled among inter-cell interference generators to achieve better total network throughput. The power-control approach is usually utilized in coordination with other solutions. As aforementioned for the time-based approaches, with power control and eNB coverage range extension, the ABS technique improves its effectiveness by reducing inter-cell interference and increases total network throughput [8, 12]. The basic principle of the power-control approach is also a trade-off in the time and space domains.

Lastly, there are hybrid approaches that exploit the benefits of aforementioned approaches by combining two or more of them together to resolve the ICI problem. One of the most important prior work is the further eICIC (FeICIC), which was introduced for LTE-A networks in the 3GPP Release 11 standard [9]. The FeICIC focuses on controlling the interference of cell-specific reference signal (CRS) resources in both the transmitter and receiver sides. On the one hand, the receiver-based FeICIC approach relies on interference cancellation to eliminate the dominant CRS source. When the receiver recognizes and estimates the strength of the dominant CRS interferer, the receiver is able to subtract it from the received signal. On the other hand, the transmitter based FeICIC relies on muting PDSCH resource elements that interfere with the MeNB's CRS elements during the RP-ABS duration.

Although existing techniques have obtained notable achievements in resolving the inter-cell interference problem, they still have a common shortcoming wherein all solutions are focused on directly attacking the inter-cell interference phenomenon to mitigate the problem. Therefore, they always encounter a trade-off issue between inter-cell interference mitigation (throughput enhancement) and resource utilization efficiency. In this work, we utilize relay-assisted communication approach based on a novel network resource availability maximization (RAmax) scheme, by which the data of the devices in the inter-cell interference area are relayed to its neighboring devices which have good signal to and from the network via D2D connection. We use the idle uplink channels or unlicensed frequencies for the D2D connection between interfered IoT terminals and relay terminals, then utilize the high quality channels of relay terminals to achieve high throughput for the interfered IoT terminals.

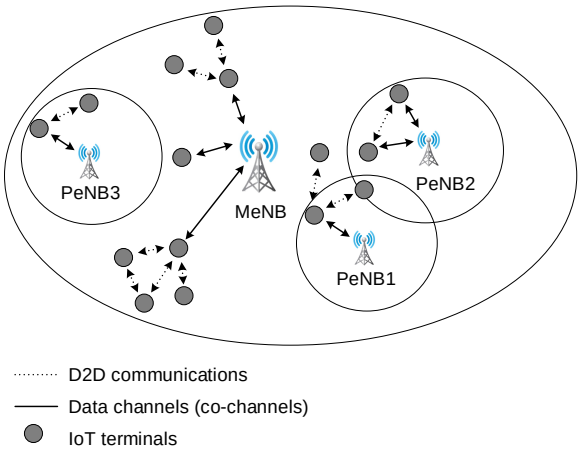

Figure 2: 5G HetNet based IoT system model.

3. Resource Availability based Relay Selection

3.1. System Model

In this paper, we consider the IoT system architecture based on 5G HetNet as an access environment, wherein D2D connection is allowed [6]. We assume the network applies a carrier aggregation-based interference mitigation technique [20] as mentioned in Section 2. The MeNB provides a common control channel for all ITs in the coverage of both MeNB and PeNBs. For wireless data transmission, MeNB and PeNBs use the same frequency channels. The controlling and signaling messages between the MeNB and the PeNBs are delivered through a X2 backhaul link (Figure 2). Accordingly, the PeNBs periodically report its current total throughput and the information of the served ITs to the MeNB. Since the MeNB and PeNBs are deployed on the same channels (i.e., co-channel deployment), it introduces inter-cell interference at the edges of the PeNBs' coverage area.

3.2. Proposed Relay Selection Procedure

We assume that ITs have already established an initial access control procedure in order to join the network, and the ITs support the ProSe-enable feature (i.e., the ITs are able to participate in proximity services standardized in the 3GPP Rel. 12 [6]). When an IT is located in ICI areas, the channel quality indicator

(CQI) decreases to a very low level, potentially introducing out-of-service behaviors. The interfered IT (iIT) in the ICI area updates its CQI to the MeNB in order to re-negotiate a proper modulation and coding scheme (MCS).

Based on our proposed procedure, the MeNB verifies the CQI reported from the iIT. If the CQI is less than a pre-defined threshold, the MeNB asks the iIT following the 3GPP ProSe standard [6] to scan its surrounding environments for a feasible D2D connection. To discover neighboring ITs, the iIT transmits a certain discovery signature (e.g., a sequence number indicator or signal patterns) in the dedicated channel for D2D discovery. Neighboring ITs in range of the discovery radius who receive the iIT's signature report its measurement results (e.g., the received power or the signal to interference plus noise ratio) to the MeNB. After mapping the neighboring ITs of iIT with its associated eNBs, the MeNB obtains a feasible list containing possible eNBs that could be selected as a reNB for the iIT. Using the proposed resource availability maximization (RAmax) function (see Section 4), the MeNB determines which eNB in the feasible list has the maximum resource availability to become the reNB. Continuously, the neighboring ITs list is filtered keeping only ITs whose associated eNB is the reNB. Based on the filtered neighboring ITs list, the MeNB elects an IT that has the maximum CQI from and to the network to be a rIT for the iIT.

After determining the appropriate pair of reNB and rIT, the MeNB initiates the initialization process for a D2D data communication between the iIT and rIT. Following 3GPP ProSe application [6], the link establishment/termination, resource allocation, and link adaptation are managed by the MeNB based on periodic measurement information reported from both the iIT and the rIT. Besides that, the MeNB orders the reNB to provide additional radio resources for the rIT according to the requirements of iIT.

3.3. An Example of the Proposed Procedure

An example model is depicted in Figure 3(a). There are 1 MeNB, 3 PeNBs, and 9 ITs numbered from 1 to 9. IT1, IT5, and IT7 are associated with PeNB1. IT2 and IT4 are associated with MeNB. IT6 and IT8 are associated with PeNB2. IT9 is associated with PeNB3. IT3 is located in the ICI area between the MeNB, PeNB1, and PeNB2. IT2, IT5, IT6 and IT7 are in the D2D discovery range of IT3.

When IT3 is located in the network, it must report its CQI to the MeNB for negotiating a connection. Since the IT3 is located within an ICI area, its CQI is very low. Therefore, the MeNB requests IT3 to take a D2D

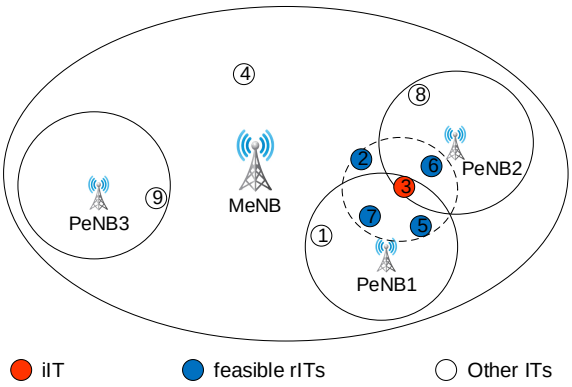

(a) An example 5G HetNet scenario consisting of 1 MeNB, 3 PeNBs, and 9 IoT terminals

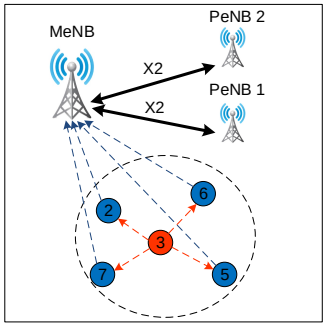

eNB	Throughput *(Mbps)*	Current users
MeNB	1280	68
PeNB1	180	12
PeNB2	160	10

IT	P_R(IT3) *(dBm)*	CQI	Associated eNB
IT2	- 78	10	MeNB
IT5	- 57	14	PeNB1
IT6	- 65	12	PeNB2
IT7	- 61	11	PeNB1

(b) Stage 1: D2D discovery and measurement reports

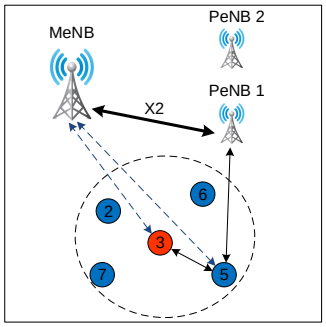

eNB	Throughput *(Mbps)*	Current users
MeNB	1280	68
PeNB1	182	13
PeNB2	160	10

IT	P_R(IT3) *(dBm)*	CQI	Associated eNB
IT2	- 78	10	MeNB
IT5	- 57	14	PeNB1
IT6	- 65	12	PeNB2
IT7	- 61	11	PeNB1

(c) Stage 2: Relay-assisted communication establishment

Figure 3: An example scenario and the two stage procedure of the proposed scheme.

discovery operation by transmitting the pre-defined discovery signal pattern. IT2, IT5, IT6, and IT7 that are in the discovery range of IT3 will receive IT3's discovery signal, and thus will calculate the received power $P_R(IT3)$ from IT3 on the D2D channel and report the results to the MeNB on the common control channel.

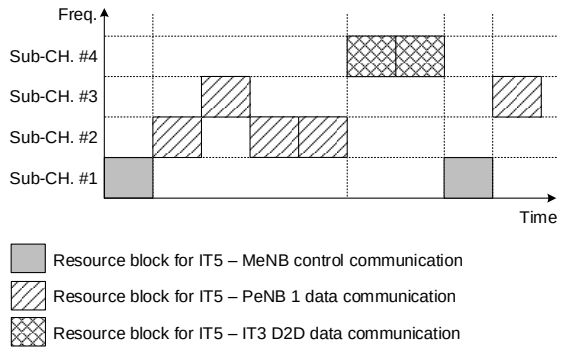

Figure 4: An example of IT5's resource allocation.

The MeNB collects the report messages and obtains the received powers $P_R(IT3)$ at IT2, IT5, IT6, and IT7 as -78 dBm, -57 dBm, -65 dBm, and -61 dBm, respectively. On the other side, the PeNB1, PeNB2, and PeNB3 periodically update their resource status (i.e., current total throughput and current served ITs) to the MeNB (Figure 3(b)).

Based on the neighboring ITs list of IT3, it can be seen that the associated eNB of IT2 is the *MeNB*, the associated eNB of IT5 and IT7 is the *PeNB1*, and IT6's associated eNB is the *PeNB2*. Therefore, the feasible list of reNB includes MeNB, PeNB1, and PeNB2. The MeNB uses the RAmax function to compare resource availability among the feasible reNBs. In this example, we assume that PeNB1 has the maximum resource availability. Hence, PeNB1 is selected as reNB for the IT3. Turning back to the neighboring ITs list of IT3, there are IT5 and IT7 whose associated eNB is PeNB1. The MeNB compares the CQI level between IT5 and IT7, and recognizes that IT5 has the best CQI value (i.e., 14). Therefore, IT5 is assigned as rIT for the IT3 (Figure 3(c)).

The MeNB controls the initialization process for a D2D data communication between IT3 and IT5. As commanded from the MeNB, PeNB1 assigns additional resources for IT5 to support IT3's requirement. From now on, IT3 can utilize relay communication to PeNB1 through a D2D link with IT5. Normally, the D2D transmission operates on the idle uplink channels or unlicensed frequency spectrum (e.g., 802.11 technology) depending on the given sensing technique in the network. An example of IT5's resource allocation is illustrated in Figure 4. The D2D communication is also managed and controlled by the MeNB to guarantee inconsiderable interference is caused by the D2D link for the network and other systems.

4. Resource Availability Maximization

In this section, we design the resource availability maximization function, RAmax, to choose an appropriate reNB for an iIT. The goal of the RAmax function is to determine which eNB has the maximum resource availability among others. The RAmax function includes three steps:

- Estimating the maximum number of ITs that an eNB can serve based on the ratio between its total throughput capacity and the summation of minimum throughput required by each current IT.
- Using the M/M/1/K/FCFS queuing model, we calculate the mean availability time of each eNB.
- Assigning the eNB which satisfies maximum availability time among the others to serve as the reNB.

4.1. RAmax Function

Consider a basic scenario where there is one MeNB and some PeNBs managed by this MeNB within its coverage. This scenario has a potential inter-cell interference problem between MeNB and PeNB at the edges of PeNBs' coverage. Assume that the grid of MeNBs is perfectly planned (e.g., OSFFR technique). Thus, (i) there is inconsiderable interference in the overlapped area among the MeNBs coverages, and (ii) the PeNBs located in the overlapped area only cause co-channel interference with their managing MeNB. Hence, the analysis results of a basic scenario could be duplicated to apply for the whole network.

Due to the fact that current LTE networks have already been using a dynamic scheduler for resource allocation, there exist a variety of possible schedulers. In this paper, we assume that the network applies the blind equal throughput (BET) scheduling technique, which is widely being used in most of state-of-the-art modern wireless networks [21, 22, 23, 24]. According to the BET, the average throughput of the *i-th* IT until time t (known as $\overline{R_i}(t)$) is equal to

$$\overline{R_i}(t) = \beta\overline{R_i}(t-1) + (1-\beta)r_i(t), \quad 0 \le \beta \le 1, \qquad (1)$$

where $r_i(t)$ is the current data rate of the *i-th* IT served by the eNB and β is a weight metric.

Let R_i^{min} denote the minimum throughput that is required by the *i-th* IT. Then the eNB must provide enough resource blocks for every IT to satisfy all below conditions simultaneously:

$$\overline{R_i}(t) \ge R_i^{min}, \forall i \qquad 1 \le i \le N, \qquad (2)$$

where N is the number of currently served ITs by the eNB.

Therefore, the maximum number of ITs (denoted by a_j) estimated at the current time t for which the *j-th* eNB can serve is determined by

$$\frac{\sum_{i=1}^{N} \overline{R_i}(t)}{\sum_{i=1}^{N} R_i^{min}(t) + (a_j - N)\overline{R^{min}}(t)} \geq 1$$
$$\Rightarrow a_j = \left\lfloor \frac{\sum_{i=1}^{N} \overline{R_i}(t) - \sum_{i=1}^{N} R_i^{min}(t)}{\overline{R^{min}}(t)} + N \right\rfloor, \tag{3}$$

where $\overline{R^{min}}(t)$ is the average minimum throughput of N number of ITs at time t.

Now, we know that after a_j, a new IT attaching to the *j-th* eNB will overload that eNB. In other words, a_j represents the current maximum service capacity of the *j-th* eNB.

To calculate the mean availability time of the *j-th* eNB, we consider the eNB as an M/M/1/K/FCFS queuing system with first-come-first-serve (FCFS) scheduling. The number of new ITs attaching to the eNB follows a *Poisson* process with mean arrival rate λ. The duration that an IT uses services via the eNB before leaving the network follows an exponential process with mean service rate μ. Since the model has memoryless property, the service capacity of the *j-th* eNB is equal to $a_j - N$ at the current time t.

According to basic queuing theory [25], the number of ITs in the eNB is a birth-death process. Therefore, the probability P_{a_j-N} that the eNB are serving $a_j - N$ number of ITs is

$$P_{a_j-N} = \frac{\rho^{a_j-N}}{\sum_{i=0}^{a_j-N} \rho^i}, \tag{4}$$

subject to $\rho = \frac{\lambda}{\mu} < 1$.

The mean number $\overline{N}$ of ITs which is being served by the eNB can be calculated as

$$\overline{N} = \frac{\rho(1 - (a_j - N + 1)\rho^{a_j-N} + (a_j - N)\rho^{a_j-N+1})}{(1-\rho)(1-\rho^{a_j-N+1})}. \tag{5}$$

Therefore, the mean availability time $\overline{T_j}$ of the *j-th* eNB from the current time t is equal to

$$\overline{T_j}(t) = \frac{\overline{N}}{\lambda(1 - P_{a_j-N})}, \tag{6}$$

subject to $\rho = \frac{\lambda}{\mu} < 1$. In the case of $\rho \geq 1$, $\overline{T_j}(t) \to \infty$.

Finally, we obtain the mean availability time $\overline{T_j}$ as follows:

$$\overline{T_j}(t) = \begin{cases} \frac{\overline{N}}{\lambda(1-P_{a_j-N})}, & \rho < 1 \\ \infty & \rho \geq 1 \end{cases}. \tag{7}$$

Based on the mean availability time analysis, we compare this value among eNBs. The *j-th* eNB that has the maximum value of the mean availability time will be assigned as reNB for iIT if it satisfies

$$\overline{T_j}(t) = \arg\max_{1 \leq i \leq M}(\overline{T_i}(t)), \tag{8}$$

where M is the total number of eNBs.

4.2. Mean Arrival Rate Refinement with Position Consideration

From Equation (7), we know that the mean availability time $\overline{T_j}$ of the *j-th* eNB depends on the mean arrival rate λ. Although the IT arrival follows a Poisson process, the arrival probability of a new IT is also in proportion with the percentage of the serving area of each eNB since the serving area of the PeNBs and the ICI areas overlay the coverage of the MeNB. In other words, when an *i-th* new IT is located in the network, it will be served by the *j-th* eNB if (❶) it is located in the serving area of the *j-th* eNB or (❷) it is located in the ICI area and successfully initiates a relay-assisted communication via D2D connection through other IT to reach the *j-th* eNB. We denote the percentage of serving area of the *j-th* eNB as s_j. To calculate the s_j values, we consider the altitude map and the signal to interference plus noise ratio (SINR) of ITs, and define the following:

- S_M: The probability that a new IT will be served by the MeNB, i.e., the IT receives the best SINR from the MeNB and the ICI level is lower than a defined threshold.
- S_{rIT_M}: The probability that a new IT will be served by the MeNB through a relay connection via a rIT, i.e., the ICI level is higher than the defined threshold and the IT successfully initiates a relay connection to the MeNB.
- S_{Pj}: The probability that a new IT will be served by the *j-th* PeNB, i.e., the IT receives the best SINR from the *j-th* PeNB and the ICI level is lower than the defined threshold.
- $S_{rIT_{Pj}}$: The probability that a new IT will be served by the *j-th* PeNB through a relay connection via a rIT, i.e., the ICI level is higher than the defined threshold and the IT successfully initiates a relay connection to the *j-th* PeNB.

- S_{Zj}: The probability that a new IT will be located in the ICI area between the MeNB and the *j-th* PeNB and the ICI level is higher than the defined threshold, or the received SINR is lower than the standard receiver sensitivity.

According to conditions ❶ and ❷, the probability s_0 of the MeNB and s_j of the *j-th* PeNB are respectively equal to

$$s_0 = S_M + \sum S_{Zj} S_{rIT_M}, \tag{9}$$

$$s_j = S_{Pj} + S_{Zj} S_{rIT_{Pj}}, \quad 1 \le j \le M, \tag{10}$$

$$\text{subject to,} \quad s_0 + \sum_{j=1}^{M} s_j = 1. \tag{11}$$

The relationship between the transmit power at the eNB and the distance from the eNB to the received IT is described by using path loss models. Nowadays, there are some popular path loss models that are widely used for predicting the behaviour of wireless cellular transmission in order to plan coverage maps, such as 3GPP, Ericsson, Okumura-Hata, COST-Hata, Erceg, Walfish, ECC-33, and Lee models [26]. To utilize the position characteristics of the received IT for estimating the serving area of the eNBs, we use the COST-Hata model [27]. The COST-Hata path loss model for urban areas is formulated as

$$\begin{aligned} P_L &= 46.3 + 33.9 log_{10} f - 13.82 log_{10} h_B - A_H + \\ &\quad + [44.9 - 6.55 log_{10} h_B] \, log_{10} d + 3, \\ A_H &= 0.8 + (1.1 log_{10} f - 0.7) h_{UE} - 1.56 log_{10} f, \end{aligned} \tag{12}$$

where

P_L*: Path loss (dB)*
h_B*: Height of eNB (m)*
h_{UE}*: Height of IT (m)*
f*: Frequency of transmission (MHz)*
d*: Distance between the eNB and IT (Km).*

Denote the transmit power of the eNB and the received power of the IT by P_T (unit: dBm) and P_R (unit: dBm), respectively. We then have,

$$P_R = P_T - P_L. \tag{13}$$

The transmit frequencies, the height of the eNB tower, the transmit power of eNB, and the IT receiver sensitivity are assumed to be constant. From Equations (12) and (13), the maximum distance where the IT still has the ability to receive the transmission signal from eNB is an exponential function of h_{UE}. In other words, it depends on the position of IT due to the landforms of the network area. Suppose that we have prior knowledge of the altitude map of the area (i.e., a map of the height above mean sea level - AMSL height). Within a given scale, we can rasterize the altitude map into a dot matrix in which each element represents the AMSL height value of the position. Figure 5 shows an example of such altitude dot matrix.

3	2	6	8	7	10	8	8	4	8
3	5	7	7	9	8	9	7	10	5
4	5	6	8	11	7	9	9	6	8
3	6	7	9	10	11	12	10	8	7
5	7	9	8	10	13	14	10	11	6
4	7	8	9	11	12	16	15	12	8
2	5	7	9	8	9	11	12	9	10
1	2	5	6	7	8	10	7	8	6

Figure 5: Example of an altitude matrix with [8 × 10] unit areas.

Let H be the matrix of the altitude map where the network is deployed,

$$H_{mn} = [x_{ij}]_{mn}, 1 \le i \le m, 1 \le j \le n, \tag{14}$$

where x_{ij} is the AMSL height at the (i, j) position. Then, the AMSL height matrix of the IT located in the network area is

$$[h_{UE}]_{mn} = H_{mn} + 1.0 J_{mn}, \tag{15}$$

where J_{mn} is the unit matrix and 1.0 is the given height of the IT in meters.

Denote the AMSL height of the MeNB and the *j-th* PeNB as x_M and x_{Pj}, respectively. Then the relative height of the IT corresponding to the AMSL height of the MeNB and *j-th* PeNB are as follows:

$$[h_{UE/M}]_{mn} = x_M J_{mn} - [h_{UE}]_{mn}, \tag{16}$$

$$[h_{UE/Pj}]_{mn} = x_{Pj} J_{mn} - [h_{UE}]_{mn}. \tag{17}$$

From Equation (12), the received power of IT from the MeNB and PeNB are respectively described as

$$[P_{R/M}]_{mn} = P_{T/M} J_{mn} - [P_L(h_{UE/M})]_{mn}, \tag{18}$$

$$[P_{R/Pj}]_{mn} = P_{T/Pj} J_{mn} - [P_L(h_{UE/Pj})]_{mn}, \tag{19}$$

and the received power of the iIT in a D2D connection from the rIT is given by

$$[P_{R/rIT}]_{mn} = P_{T/rIT} J_{mn} - [P_L(H)]_{mn}. \tag{20}$$

$$x_{ij}^{(1)} = \begin{cases} 1, & \text{if} \begin{cases} SINR(x_{ij}) \geq \varepsilon \\ P_{R/M}(x_{ij}) \geq \gamma \\ P_{R/M}(x_{ij}) = \arg\max\limits_{1 \leq t \leq M} \left\{ P_{R/M}(x_{ij}), P_{R/Pt}(x_{ij}) \right\} \end{cases} \\ 0, & \text{otherwise} \end{cases} \tag{21}$$

$$x_{ij}^{(2)} = \begin{cases} 1, & \text{if} \begin{cases} SINR(x_{ij}) \geq \varepsilon \\ P_{R/Pk}(x_{ij}) \geq \gamma \\ P_{R/Pk}(x_{ij}) = \arg\max\limits_{1 \leq t \leq M} \left\{ P_{R/M}(x_{ij}), P_{R/Pt}(x_{ij}) \right\} \end{cases} \\ 0, & \text{otherwise} \end{cases} \tag{22}$$

$$x_{ij}^{(3)} = \begin{cases} 1, & \text{if} \begin{cases} SINR(x_{ij}) \geq \varepsilon \\ P_{R/rIT}(x_{ij}) \geq \gamma \end{cases} \\ 0, & \text{otherwise} \end{cases} \tag{23}$$

$$x_{ij}^{(4)} = \begin{cases} 1, & \text{if} \begin{cases} SINR(x_{ij}) < \varepsilon \\ P_{R/Pk}(x_{ij}) = \arg\max\limits_{1 \leq t \leq M} \left\{ P_{R/Pt}(x_{ij}) \right\} \\ P_{R/M}(x_{ij}) = \arg\max\limits_{1 \leq t \leq M} (\left\{ P_{R/M}(x_{ij}), P_{R/Pt}(x_{ij}) \right\} \setminus P_{R/Pk}(x_{ij})) \end{cases} \\ 0, & \text{otherwise} \end{cases} \tag{24}$$

Now, to calculate the positions at which an IT can (or cannot) associate with the MeNB, PeNBs, and rIT according to the conditions ❶ and ❷, we first define four conditional functions $x_{ij}^{(1)}, x_{ij}^{(2)}, x_{ij}^{(3)}, x_{ij}^{(4)}$ as shown in Equations (21), (22), (23), and (24), respectively, where γ is the standard receiver sensitivity of an IT, and ε is the SINR threshold of the received signal at the IT.

Then, the number of positions at which an IT can associate with the MeNB, PeNBs, and rIT (denoted by V_M, V_{Pk}, V_{rIT}, respectively) are

$$V_M = \sum_{i=1}^{m} \sum_{j=1}^{n} x_{ij}^{(1)}, \tag{25}$$

$$V_{Pk} = \sum_{i=1}^{m} \sum_{j=1}^{n} x_{ij}^{(2)}, \tag{26}$$

$$V_{rIT} = \sum_{i=1}^{m} \sum_{j=1}^{n} x_{ij}^{(3)}; \tag{27}$$

and number of positions at which an IT is in the ICI area between the MeNB and the *k-th* PeNB but cannot establish a relay connection to any eNB is

$$V_{Zk} = \sum_{i=1}^{m} \sum_{j=1}^{n} x_{ij}^{(4)}, \tag{28}$$

Therefore, $S_M, S_{Pj}, S_{Zj}, S_{rIT_M}$, and $S_{rIT_{Pj}}$ are respectively given by

$$S_M = \frac{V_M}{V_M + \sum V_{Pj} + \sum V_{Zj}}, \tag{29}$$

$$S_{Pj} = \frac{V_{Pj}}{V_M + \sum V_{Pj} + \sum V_{Zj}}, \tag{30}$$

$$S_{Zj} = \frac{V_{Zj}}{V_M + \sum V_{Pj} + \sum V_{Zj}}, \tag{31}$$

$$S_{rIT_M} = \frac{\sum_{i=1}^{m} \sum_{j=1}^{n} (x_{ij}^{(1)} \cap x_{ij}^{(3)})}{V_M + \sum V_{Pj} + \sum V_{Zj}}, \tag{32}$$

$$S_{rIT_{Pj}} = \frac{\sum_{i=1}^{m} \sum_{j=1}^{n} (x_{ij}^{(2)} \cap x_{ij}^{(3)})}{V_M + \sum V_{Pj} + \sum V_{Zj}}. \tag{33}$$

Figure 6 illustrates an example of service prediction map, calculated by Equations (29)-(33), based on a given altitude map. The probabilities s_0, s_j in Equations (9) and (10) are updated by the formulas for S_M, S_{Pj}, S_{Zj}, S_{rIT_M}, and $S_{rIT_{Pj}}$.

Finally, the mean availability time $\overline{T_j}$ of the *j-th* eNB in Equation (7) is updated as follows

$$\overline{T_j}(t) = \begin{cases} \frac{\overline{N}}{\lambda s_j (1 - P_{a_{j-N}})}, & \rho < 1 \\ \infty & \rho \geq 1 \end{cases}. \tag{34}$$

5. Performance evaluation

To evaluate the effectiveness of the proposed algorithm, we have built a typical network topology that

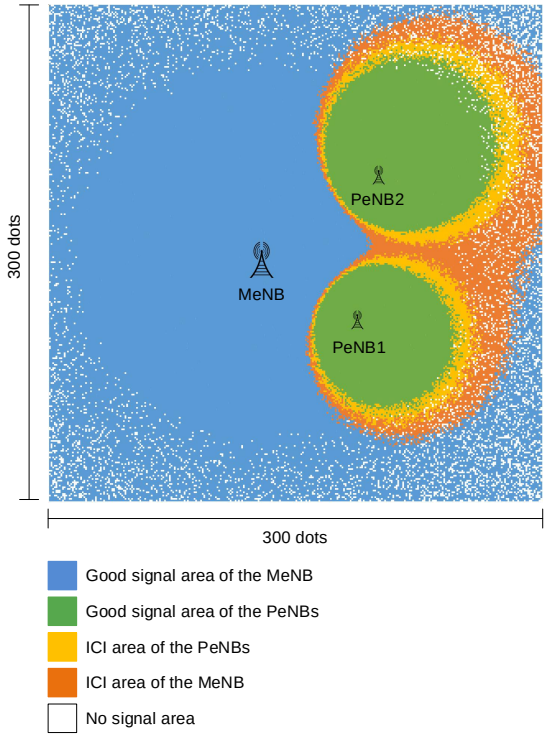

Figure 6: An example service prediction map of the experimental altitude matrix [300 × 300].

consists of a MeNB and five PeNBs. Although we consider a single MeNB cell for evaluation, as aforementioned in Section 3, this cell can be duplicated to expand and represent for the whole network. Moreover, 300 Monte Carlo experiments have been performed, wherein the positions of PeNBs and ITs are randomly deployed for each experiment in order to create various networking scenarios. The parameters used for our simulation study are summarized in Table 1. We simulated the network on a map with dimensions of 3000x3000 m^2, where each matrix element covers a 10x10 m^2 unit area. The height of the eNB tower is set to 35 m, excluding AMSL height of the position. The given landform map is rasterzied into a dot matrix with a dimension of 300x300 unit areas. The minimum throughput required by an IT that must be guaranteed is configured to be at least 100 kbps. To evaluate the improvements of the proposed algorithm, we compared the throughput of each eNB and the whole network for three different algorithms: CA technique, ABS technique, and the proposed algorithm, RAmax. Also, to evaluate the effectiveness of the proposed algorithm, we consider the number of ITs that the network can serve simultaneously and the number of assigned resource blocks for each IT in the ICI area as our evaluation metrics.

Table 1: Simulation parameters.

Parameter	Value
Network layout	1 MeNBs and 5 PeNBs
Deployment scenario	co-channel HetNet
Cumulative ITs	600 devices
Mean arrive rate (λ)	1.2 IT/s
Mean service rate (μ)	0.5 IT/s
Transmit power of MeNB	36 dBm
Transmit power of PeNB	24 dBm
Carrier frequency	2000 MHz
Bandwidth	1.4 MHz for eMTC [28]
Transmit power of IT	21 dBm
Receiver sensitivity (γ)	-107.5 dBm [29]
Path loss model	COST-Hata
Landforms map	Urban area

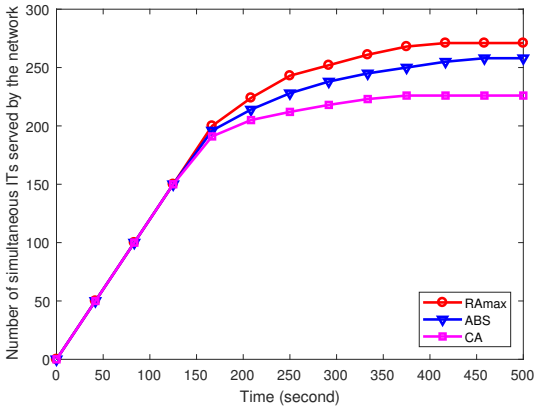

Figure 7: The number of simultaneous IoT terminals (ITs) served by the network.

Figure 7 shows the number of simultaneous ITs served by the network. When the number of ITs arriving at the network is small, up until around first 200 ITs including the interfered ITs, all the ITs are served by the network based on the the BET schedule [22] since all of the eNBs still have enough available resources. However, after that point as new ITs attach continuously to the network, the eNBs' capacities approach close to their maximum limit. Therefore, some of the new ITs that arrived at the network are dropped due to lack of available network resources. The maximum number of simultaneous ITs that the network can serve by using RAmax, ABS, and CA techniques are 271, 257, and 226, respectively. The result shows that the proposed algorithm increases by 19.91% and 5.45% of the number of ITs that can be served by the network simultaneously in comparison to applying ABS and CA techniques, respectively, which means that RAmax algorithm improves the resource availability of the net-

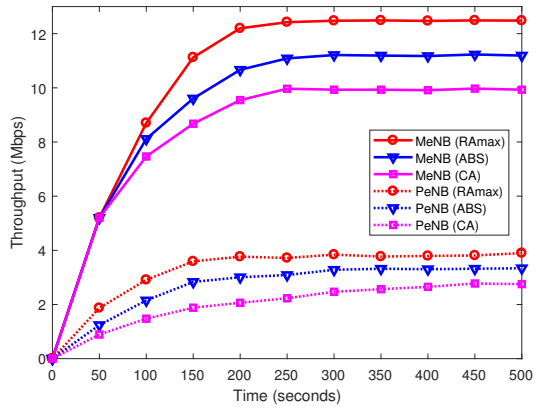

Figure 8: Throughput of the macro eNB and average throughput of pico eNBs for three different algorithms ABS, CA, and RAmax.

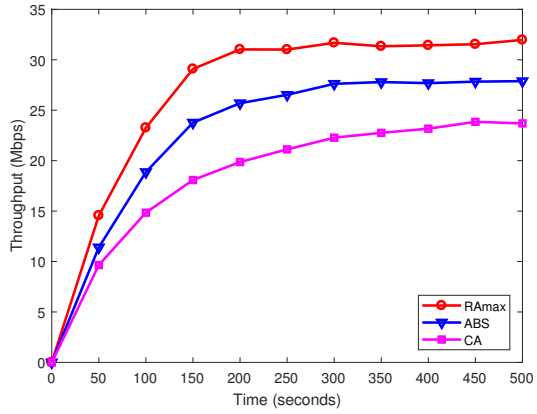

Figure 9: Total aggregate throughput of the network for three different algorithms ABS, CA, and RAmax.

work.

Figures 8 and 9 show the real-time throughput of the eNBs and the whole network among the proposed algorithm and other techniques. The proposed algorithm increased the total throughput by up to 43.96% and 17.07% in comparison to applying ABS and CA techniques, respectively, due to ICI avoidance and higher spectrum usage efficiency by relaying communication via an ITs with good signal. Although the proposed algorithm creates a little extra overhead (i.e., D2D discovery, initial D2D link establishment, and control messages), the average total network throughput in saturation condition still increases significantly from 22.39 Mbps (CA) and 27.29 Mbps (ABS) to 31.43 Mbps within 1.4 MHz bandwidth following the 3GPP Rel. 13 for eMTC [28].

Figure 10 plots performances of iITs located in the ICI area in terms of the number of assigned resource blocks (Figure 10a), the energy consumption during each TTI (Figure 10b), and the 3GPP-based code rate [30] (Figure 10c).

In Figure 10a, in addition to gaining higher network throughput, the average number of resource blocks assigned to the iIT based on the RAmax is also lower than the ABS and CA techniques. This is because, without the proposed algorithm, the network has to assign more resource blocks to compensate the iIT for its low channel quality. However, within the proposed algorithm, the iIT relays its communication via a D2D link through its neighboring IT that has a good quality channel. Therefore, the number of resource block that the network has to assign to satisfy the requirements of an iIT is decreased relatively by utilizing the better channel quality of the rIT. Simulation result shows that the average number of assigned resource blocks for the iIT decreases from 4.14 RB/UE (CA) and 2.36 RB/UE (ABS) to 1.29 RB/UE. The lower number of resource blocks reflects the lower transmission power consumption and higher throughput (as represented in Figures 8 and 9). Moreover, the length of the boxes illustrates that the number of assigned resource blocks is diverse among iITs in CA algorithm. Meanwhile, ABS algorithm achieves better result and RAmax obtains the best result compared to CA algorithm.

Under the assumption that the D2D connection utilizes the unlicensed bands of IEEE 802.11ac technology, the time-average energy per one transmission time interval (TTI) consumed by the iIT to transmit its data is lower than the CA technique and similar to the ABS technique. Based on our model, the energy consumption is the summation of the transmission power of the bidirectional D2D link between the iIT and rIT and the transmission power of rIT uplink to the reNB. The result shows that the proposed algorithm still reduces the transmission power for ITs located in the ICI area by about 44.15% in comparison with the CA technique (see Figure 10b).

As a result, due to the interference avoidance ability, the ITs located in the ICI area within our proposed algorithm get higher code rates. Standardized by 3GPP, the code rate depends on the modulation and coding scheme (i.e., the channel quality) and the number of assigned resource blocks for each IT. The code rate can be defined as how effectively data can be transmitted in 1 *ms* transport block [30]. The numerical results are shown in Figure 10c. Although the code rate improvement varies a lot among iITs, the corresponding effect is generally positive when applying the proposed algorithm. Average code rate of the ITs are 0.401, 0.379, and 0.302 given by RAmax, ABS, and CA algorithms,

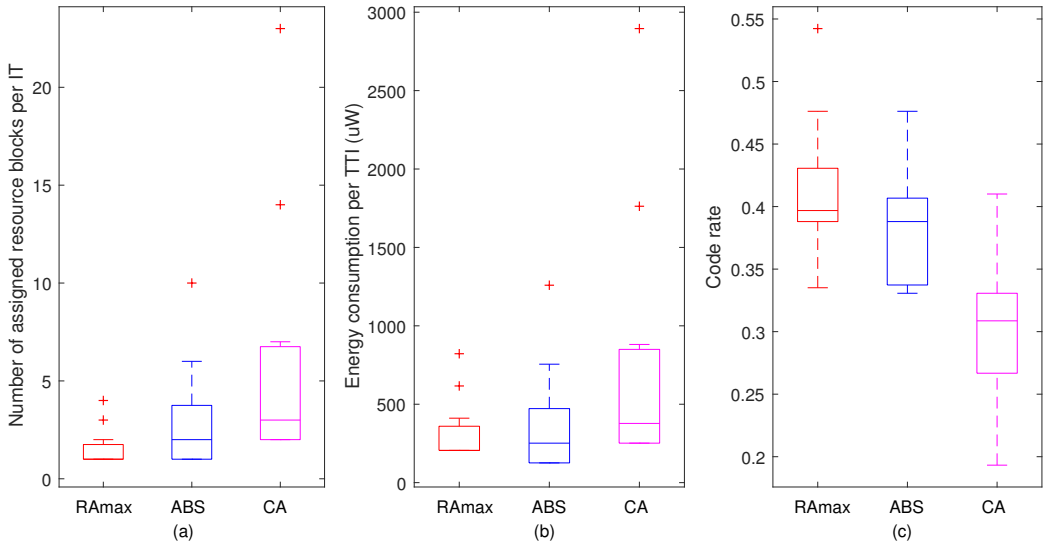

Figure 10: Performances of IoT terminals (ITs) located in the inter-cell interference area: a) The number of assigned resource blocks; b) The energy consumption during each TTI; and c) The code rate.

respectively.

6. Discussion

In building up the proposed solution, there are three participants including the network operator (represented by the MeNB and PeNBs), the iIT, and the rIT. Clearly, the network operator benefits more when they participate in this solution. Due to the radio resource usage efficiency, the network operator has more free available resources to support the new ITs. Moreover, through the high quality channel of the rIT, data rate from an iIT increases significantly, which then gives the network operator more revenue. However, it is not obvious whether the rIT, by forwarding the data traffic of other iITs and spending energy to do so, will benefit from using our proposal. To encourage the IT to participate in the proposed scheme, Tehrani *et.al.* [5] suggested that the network operator can offer incentives such as a discount voucher or cashback to the IT's billing account based on the data volume it supported for other devices. Although the exact incentive mechanism is left to be determined by the network operator, we believe that the interests of both the network operator and the ITs can be met if the network achieves significant improvement in resource availability and throughput.

In this paper, we proposed an effective algorithm to select a pair of an eNB and an IT to provide relay-assisted communications for the ITs with poor signals in the ICI area to connect to the network. The advantages are represented by the network throughput improvement and a reduction in the number of assigned resource block. However, the proposed algorithm also has some limitations. Because the algorithm utilizes a D2D link between ITs to establish a relay connection to the network, it causes more transmission delay for the iIT. Furthermore, in the scope of this paper, the authors limited the study to an one-hop relay connection in order to avoid significant extra latency due to D2D links. However, we may need to consider multi-hop relaying for future research to improve the effectiveness. Lastly, the user privacy and security are not considered and are assumed to be provided based on the ProSe model standardized in 3GPP 22.803 [6].

7. Conclusion and Future Work

The 5G heterogeneous network is expected to provide promising infrastructure for ubiquitous and high data rate communication in the upcoming Internet of Things. However, the signals of IoT terminals located at the edge of the Pico eNBs' coverage are known to suffer from significant inter-cell interference from other PeNBs or MeNBs due to the co-channel deployment model of 5G HetNets. On the other hand, device-to-device communication has already been standardized in 3GPP Rel.12 for LTE-Advanced networks, and is developing to be more widely acceptable in the 5G heterogeneous networks where the IoT terminals are located

densely, especially in urban areas. In this paper, we proposed a novel algorithm which selects the most appropriate pair of IoT terminal and its associated eNodeB with good signals to provide a relay-assisted communication for the IoT terminals with poor signals in the inter-cell interference area. The results show that the total network throughput and the number of simultaneously served IoT terminals increases up to 43.96% and 17.07%, respectively. Moreover, the average transmission energy of IoT terminals consumed during each TTI decreases by 44.15%. As a future research direction, we plan to develop an algorithm that utilizes multi-hop relaying in order to provide better connection availability and support more IoT terminals simultaneously.

Acknowledgements

This research was supported by Basic Science Research Program through the National Research Foundation of Korea (NRF) funded by the Ministry of Science and ICT (NRF-2017R1A2B4009802 and NRF-2017R1A4A1015675).

References

[1] Nortel, Vodafone, Open and closed access for Home NodeBs, Tech. Rep. #44 R4-071231, 3GPP TSG RAN Working Group 4 (2007).

[2] A. Daeinabi, K. Sandrasegaran, X. Zhu, Survey of intercell interference mitigation techniques in LTE downlink networks, in: IEEE Australasian Telecommunication Networks and Applications Conference (ATNAC), 2012, pp. 1–6.

[3] W. Na, N.-N. Dao, S. Cho, Reliable multicasting service for densely deployed military sensor networks, International Journal of Distributed Sensor Networks 11 (8) (2015) 341912.

[4] A. Orsino, A. Ometov, G. Fodor, D. Moltchanov, L. Militano, S. Andreev, O. N. Yilmaz, T. Tirronen, J. Torsner, G. Araniti, et al., Effects of Heterogeneous Mobility on D2D-and Drone-Assisted Mission-Critical MTC in 5G, IEEE Communications Magazine 55 (2) (2017) 79–87.

[5] M. N. Tehrani, M. Uysal, H. Yanikomeroglu, Device-to-device communication in 5G cellular networks: challenges, solutions, and future directions, IEEE Communications Magazine 52 (5) (2014) 86–92.

[6] Feasibility study for Proximity services (ProSe) (Release 12), 3GPP Technical Report 22.803 v.12.2.0 (2013).

[7] Comparison of time-Domain eICIC solutions, 3GPP R1-104661 (2010).

[8] Summary of the description of candidate eICIC solutions, 3GPP R1-104968 (2010).

[9] J. Acharya, L. Gao, S. Gaur, Release 11 Further Enhanced ICIC: Transceiver Processing, Heterogeneous Networks in LTE-Advanced (2014) 133–148.

[10] M. S. Ali, An overview on interference management in 3GPP LTE-advanced heterogeneous networks, International Journal of Future Generation Communication and Networking 8 (1) (2015) 55–68.

[11] M. S. Ali, On the Evolution of Coordinated Multi-Point (CoMP) Transmission in LTE-Advanced, International Journal of Future Generation Communication and Networking 7 (4) (2014) 91–102.

[12] G. Boudreau, J. Panicker, N. Guo, R. Chang, N. Wang, S. Vrzic, Interference coordination and cancellation for 4G networks, IEEE Communications Magazine 47 (4) (2009) 74–81.

[13] V. Garcia, Y. Zhou, J. Shi, Coordinated multipoint transmission in dense cellular networks with user-centric adaptive clustering, IEEE Transactions on Wireless Communications 13 (8) (2014) 4297–4308.

[14] D. Lee, H. Seo, B. Clerckx, E. Hardouin, D. Mazzarese, S. Nagata, K. Sayana, Coordinated multipoint transmission and reception in LTE-advanced: deployment scenarios and operational challenges, IEEE Communications Magazine 50 (2) (2012) 148–155.

[15] K. I. Pedersen, Y. Wang, S. Strzyz, F. Frederiksen, Enhanced inter-cell interference coordination in co-channel multi-layer LTE-advanced networks, IEEE Wireless Communications 20 (3) (2013) 120–127.

[16] N. Saquib, E. Hossain, D. I. Kim, Fractional frequency reuse for interference management in LTE-advanced HetNets, IEEE Wireless Communications 20 (2) (2013) 113–122.

[17] J. Xie, C. Xiaogang, Y. Zhu, H. Yang, L. Dai, A Novel Method to Solve CRS/PDSCH RE Collision in Joint Transmission in LTE-A, in: IEEE International Conference on Connected Vehicles and Expo (ICCVE), 2012, pp. 66–70.

[18] Y. Cao, Y. Wen, X. Meng, W. Xu, Performance Evaluation with Improved Receiver Design for Asynchronous Coordinated Multipoint Transmissions, Chinese Journal of Electronics 25 (2) (2016) 372–378.

[19] W. Zirwas, Opportunistic comp for 5G massive MIMO multi-layer networks, in: The 19th VDE International ITG Workshop on Smart Antennas (WSA 2015), 2015, pp. 1–7.

[20] M. Iwamura, K. Etemad, M.-H. Fong, R. Nory, R. Love, Carrier aggregation framework in 3GPP LTE-advanced [WiMAX/LTE Update], IEEE Communications Magazine 48 (8) (2010) 60–67.

[21] N.-N. Dao, M. Park, J. Kim, S. Cho, Adaptive MCS selection and resource planning for energy-efficient communication in LTE-M based IoT sensing platform, PloS one 12 (8) (2017) e0182527.

[22] F. Capozzi, G. Piro, L. A. Grieco, G. Boggia, P. Camarda, Downlink packet scheduling in LTE cellular networks: Key design issues and a survey, IEEE Communications Surveys & Tutorials 15 (2) (2013) 678–700.

[23] P. Kela, J. Puttonen, N. Kolehmainen, T. Ristaniemi, T. Henttonen, M. Moisio, Dynamic packet scheduling performance in UTRA long term evolution downlink, in: The 3rd IEEE International Symposium on Wireless Pervasive Computing (ISWPC), 2008, pp. 308–313.

[24] N.-N. Dao, J. Lee, D.-N. Vu, J. Paek, J. Kim, S. Cho, K.-S. Chung, C. Keum, Adaptive resource balancing for serviceability maximization in fog radio access networks, IEEE Access 5 (2017) 14548–14559.

[25] V. G. Kulkarni, Modeling and analysis of stochastic systems, CRC Press, 2016.

[26] M. Alshami, T. Arslan, J. Thompson, A. Erdogan, Evaluation of path loss models at WiMAX cell-edge, in: The 4th IEEE IFIP International Conference on New Technologies, Mobility and Security (NTMS), 2011, pp. 1–5.

[27] N. Nkordeh, A. Atayero, F. Idachaba, O. Oni, LTE Network Planning using the Hata-Okumura and the COST-231 Hata Pathloss Models, in: The World Congress on Engineering, 2014, pp. 1–5.

[28] M. Lauridsen, I. Kovács, P. E. Mogensen, M. Sørensen, S. Holst,

Coverage and capacity analysis of lte-m and nb-iot in a rural area, in: The 84th IEEE Vehicular Technology Conference (VTC Fall), 2016, pp. 1–5.

[29] H. Holma, A. Toskala, WCDMA for UMTS: HSPA evolution and LTE, John Wiley & Sons, 2010.

[30] Evolved Universal Terrestrial Radio Access (E-UTRA); Physical Layer Procedures, 3GPP Technical Specification 36.213 v.11.4.0 (2010).